Radial Distribution of Valence Neutrons from Elastic Electron Scattering

I. Sick*
Department of Physics, University of Basel, Basel, Switzerland

and

J. B. Bellicard, J. M. Cavedon, B. Frois, M. Huet, P. Leconte, A. Nakada, Phan Xuan Hô, and S. Platchkov
Département de Physique Nucléaires et Hautes Energies, Centre d'Etudes Nucléaires de Saclay, Gif-sur-Yvette, France

and

P. K. A. deWitt Huberts and L. Lapikás
Institute for Nuclear Physics Research, Amsterdam, The Netherlands
(Received 22 March 1977)

Cross sections for elastic scattering of 175–300-MeV electrons by the nuclear magnetization current density of ^{87}Sr have been measured. The results are used to determined the shape of the radial wave function of the valence neutron shell. The experiment yields a rms radius of $1g_{9/2}$ neutrons that is 0.31 ± 0.04 fm smaller than predicted by density-dependent Hartree-Fock theory.

Elastic electron scattering and muonic x-ray experiments provide a clean and precise determination of the radial distribution of protons in nuclei. A comparable probe interacting specifically with neutrons is not available, and less clean methods have been used to obtain information on neutron densities $\rho_n(r)$. These include Coulomb energy differences,[1] pick-up reactions,[2] α, p, π scattering,[3] π total cross sections,[4] $K^-, \bar{p}$ absorption,[5] and π, ρ^0 photoproduction.[6] These methods do not allow a measurement of the entire distribution $\rho_n(r)$; they are sensitive to individual shells, or to $\rho_n(r)$ at large radii only. More importantly, they involve strongly interacting probes; the extraction of nuclear properties then depends on assumptions concerning the reaction mechanism. The validity of these assumptions is hard to assess. Judging from the dispersion of results obtained, the experimental uncertainty in the radial extension of neutrons still exceeds the predicted difference between proton and neutron radii of a few percent.[7]

We have used magnetic electron scattering (as opposed to scattering by the charge density) to measure the valence-neutron radial wave functions.[8] Whereas this measurement also determines only part of $\rho_n(r)$, it is the first one to do it without the ambiguities involved with strongly interacting probes.

We consider elastic magnetic scattering of the highest multipolarity $\lambda = 2j$ from an even-odd spin-j nucleus. Assume that the spin $j = l + \frac{1}{2}$ of the unpaired nucleon is the highest one of all filled shells, and that this nucleon is, to a reasonable purity, in a single-particle state. Then, the cross section for magnetic scattering of multipolarity λ, $\sigma_{M\lambda}$, can be separated from that for charge scattering and other magnetic multipoles $\lambda' < \lambda$ over a large range of momentum transfer q.[9,10] Also, $\sigma_{M\lambda}$ depends on the distribution of intrinsic spin magnetization only. In contrast to the case $\lambda' < \lambda$ the influence of valence configuration mixing on $\sigma_{M\lambda}$ is expected to be very small, since the relevant core excitations involve two-particle–two-hole states of an energy of at least $2\hbar\omega$ in the oscillator shell model and spins $j' > j$ only.[10]

For the present case, $\sigma_{M\lambda}$ is determined almost exclusively by the unpaired nucleon's radial wave function $R(r)$. In the plane-wave Born approximation we obtain

$$\sigma_{M\lambda} = \sigma_{\mathrm{Mott}}\, \eta(\tfrac{1}{2} + \tan^2\tfrac{1}{2}\theta) \times F_N^{\,2}(q) F_{\mathrm{c.m.}}^{\,2}(q) F_{M\lambda}^{\,2}(q), \quad (1)$$

where σ_{Mott} is the cross section for a pointlike nucleus, η is the recoil factor,[10] θ is the scattering angle, F_N is the nucleon magnetic form factor, and $F_{\mathrm{c.m.}}$ is the center-of-mass form factor.[10] For the $1g_{9/2}$ nucleons considered below, the $M9$ form factor is

$$F_{M9}(q) = \alpha_9 \mu_N \frac{q}{M_N} \frac{3 \cdot 7}{(11 \cdot 13 \cdot 17/5)^{1/2}} \times \int_0^\infty R^2(r) j_8(qr) r^2\, dr\,. \quad (2)$$

Here α_9 is the ratio of the many-body to single-

particle matrix element of the $M9$ operator, $\langle \frac{9}{2}^+ \| \hat{T}_9^{\text{mag}} \| \frac{9}{2}^+ \rangle / \langle 1g_{9/2} \| \hat{T}_9^{\text{mag}} \| 1g_{9/2} \rangle$; M_N and μ_N are the nucleon mass and magnetic moment. The above equations serve to demonstrate the relation between $R(r)$ and $F(q)$; for the actual analysis of the data the more exact distorted-wave Born approximation will be used.

The experiment was carried out on ^{87}Sr, whose ground state has a $1g_{9/2}$ neutron hole configuration; the $l=4$ spectroscopic factor is close to 1,[11] and shells with $j > \frac{9}{2}$ start to get filled only for $A \gtrsim 120$. The nine $1g_{9/2}$ neutrons give a large contribution ($\sim 30\%$) to the total neutron rms radius as a result of the surface-peaked nature of $R(r)$.

The Centre d'Etudes Nucléaires de Saclay linear accelerator and HE1 end station[12] were used. Electrons of 175–300 MeV energy ($\Delta E/E \simeq 5 \times 10^{-4}$) were scattered at 155° from ^{87}Sr (93% enriched) and ^{88}Sr targets. The beam current of ~ 12 μÅ was integrated with a Faraday cup. The absolute efficiency of the SP900 spectrometer and associated focal-plane equipment[12,13] was calibrated relative to ^{12}C elastic cross sections[14] at low q. The ^{87}Sr and ^{88}Sr total cross sections were measured with this setup; the contribution of charge scattering was measured at 500 MeV and forward angles and subtracted.

The resulting magnetic cross sections are shown in Fig. 1. To a good approximation (see below) these cross sections are due to $M9$ scattering only, since the lower-multipole form factors fall off very quickly at high q. Also shown in Fig. 1 is a distorted-wave Born-approximation[15] prediction for a density-dependent Hartree-Fock (DDHF) $1g_{9/2}$ wave function[16] and $\alpha_9 = 0.85$. This DDHF calculation is based on an effective NN interaction derived from the Reid soft-core potential. Given that σ^{DDHF} falls off too quickly, the radial size of $R^{\text{DDHF}}(r)$ must be too large by a considerable amount. Since DDHF theory correctly predicts the total charge radius, this is a very surprising observation.

Figure 1 also shows a curve for $R^{\text{WS}}(r)$ calculated in a Woods-Saxon well. {We use a WS potential $V(r) = V_0/[1+\exp((r-R)/z)]$, with $R = r_0(A-1)^{1/3}$, together with surface spin-orbit and Coulomb terms.} The WS radius parameter $r = 1.175$ fm has been fitted to the data while the potential depth $V_0 = 53$ MeV was adjusted to reproduce the neutron separation energy $E_s = 8.42$ MeV. The surface thickness $z = 0.65$ fm was determined by fitting our ^{88}Sr charge cross sections with the charge density ρ^{WS} obtained from the single-particle radial wave functions calculated for a WS potential; this procedure is based on DDHF results[17] that yield nearly the same surface thickness for the effective potentials seen by nucleons in the different occupied shells. In the fit of the magnetic cross sections, both $M7$ and $M9$ contributions were allowed for, yielding $\alpha_9 = 0.85 \pm 0.05$ and an $\alpha_7 < 0.83$ compatible with zero. The α_9 being close to 1 confirms that the $M9$ data can be interpreted in terms of WS or DDHF single-particle wave functions. The resulting square of the radial wave function is shown in Fig. 2.

As a particularly relevant test of theory an in-

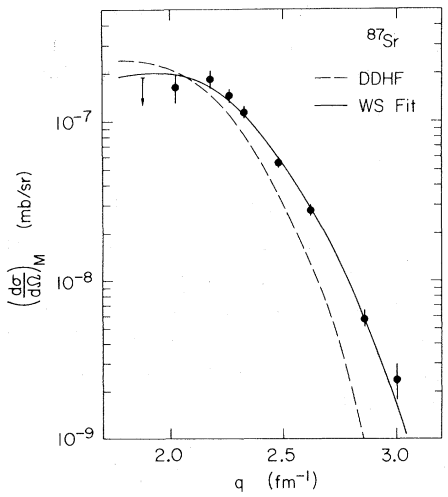

FIG. 1. Magnetic cross sections as a function of effective momentum transfer. The χ^2 for the WS fit is 9.5.

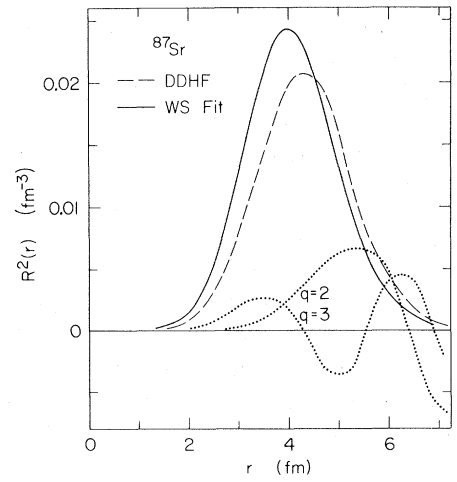

FIG. 2. $1g_{9/2}$ neutron radial wave functions. The dotted curves represent $j_8(qr)r^2$ [Eq. (2)] for $q = 2$ and 3 fm^{-1}, and show that the experiment is mainly sensitive to $R(r)$ between 2.5 and 6.5 fm.

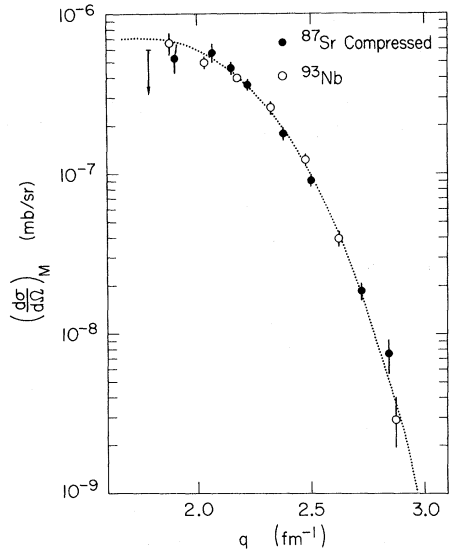

FIG. 3. $M9$ cross sections for $1g_{9/2}$ protons in ^{93}Nb, and $1g_{9/2}$ neutrons in ^{87}Sr plotted on compressed q scale. The q dependence of the WS fit to ^{93}Nb (dotted) was used for interpolation between pairs of Nb data points only.

dependent interpretation of the data directly compares proton and neutron radii by a comparison of proton and neutron $M9$ form factors. For this purpose we used our $M9$ cross sections[18] of ^{93}Nb, a nearby nucleus having an unpaired $1g_{9/2}$ proton. If proton and neutron $1g_{9/2}$ wave functions are similar in shape (as supported by DDHF and WS calculations) we may assume that they differ essentially in a change in radial scale by a factor β,

$$R_p(r) = R_n(\beta r)\beta^{3/2}, \tag{3}$$

the factor $\beta^{3/2}$ being used to keep $R_p(r)$ normalized. Then

$$F_p(q) = F_n(q/\beta)\mu_p\,\alpha_p/\mu_n\,\alpha_n. \tag{4}$$

A comparison of F_p and F_n then yields β independent of specific model assumptions concerning $R(r)$.[19]

Figure 3 shows the $M9$ cross sections[18] for ^{93}Nb; also shown are the renormalized ^{87}Sr data [Eq. (4)] plotted on a compressed q scale. The χ^2 between interpolated Nb and compressed Sr data is 18. The Nb and Sr points clearly define a unique $M9$ curve, hereby justifying our assumption, Eq. (3), that proton and neutron $1g_{9/2}$ radial wave functions differ essentially by a compression of the radial scale. The resulting compression factor is $\beta = 0.954 \pm 0.006$.

Table I collects the $1g_{9/2}$ rms radii. The DDHF calculation reproduces the experimental separation energies within 1–2 MeV only; this deviation essentially influences the large-r ($r > 6.5$ fm) falloff of $R(r)$, without much change for $r < 6.5$ fm. The rms radii denoted in Table I by an asterisk,

$$r_{\mathrm{rms}}^{\mathrm{DDHF}*} = r_{\mathrm{rms}}^{\mathrm{DDHF}} + \frac{\partial r_{\mathrm{rms}}}{\partial E_s}\left(E_s^{\mathrm{exp}} - E_s^{\mathrm{DDHF}}\right),$$

calculated using $\partial r_{\mathrm{rms}}/\partial E_s$ from WS calculations, correct for the influence on r_{rms} of this incorrect large r behavior. Similarly, the compression does not quite properly transform the Sr/Nb asymptotic tails (to which the present experiment is not sensitive). For the comparison of rms radii, this effect should be corrected for, and leads to the β^* quoted in Table I. The DDHFB prediction[20] also shown comes from a Hartree-Fock-Bogolyubov calculation that uses a phenomenological NN interaction. It gives charge rms radii 0.4% smaller than experiment; as compared to DDHF predictions both the DDHFB $1g_{9/2}$ neutron and proton radii are in somewhat better agreement with experiment.

From Table I we conclude that DDHG theory predicts neutron wave functions with an rms radius 6.3% (0.31 ± 0.04 fm) too large. The direct determination of the p-n difference in rms radius (β^*) indicates that in comparison to protons in ^{93}Nb DDHF theory predicts neutrons 3.7% (0.18 ± 0.03 fm) too far outside. This discrepancy with one of the best calculations available is very surprising, since proton and neutron densities are believed to be strongly coupled; protons are mostly responsible for the self-consistent mean field

TABLE I. $1g_{9/2}$ point-nucleon rms radii (fm) and ratios. [$\beta^* = 0.962 \pm 0.006$ is the corrected compression factor (see text).]

Nucleus	WS fit	DDHF	DDHFB	DDHF*	DDHFB*
^{87}Sr	4.655 ± 0.040	4.893	4.845	4.968	4.837
^{93}Nb	4.834 ± 0.035	4.953	4.943	4.973	4.945
^{87}Sr/^{93}Nb	0.963 ± 0.012			0.999	0.978

seen by neutrons, and vice versa. (Note that DDHF theory reproduces experimental charge radii of ^{87}Sr and ^{93}Nb within 0.2%.) It should be added, however, that experimental charge radii have been used for adjustments of the density dependence of the effective *NN* force, whereas no such information on neutrons was available. Our results also contradict the often cited expectation that, for nuclei with $N > Z$, the excess neutrons should lead to a distinct neutron halo.

The authors would like to thank Dr. X. Campi, Dr. J. Decharge, Dr. T. W. Donnelly, and Dr. D. Gogny for discussions and communication of results before publication, and D. Goutte for help during the experiment.

*Work supported by the Swiss National Science Foundation.

[1]J. A. Nolen and J. P. Schiffer, Annu. Rev. Nucl. Sci. 19, 471 (1969).

[2]G. D. Jones, J. L. Durell, J. S. Lilley, and W. R. Phillips, Nucl. Phys. A230, 173 (1974); J. P. Schiffer and H. J. Körner, Phys. Rev. C 8, 841 (1973).

[3]A. M. Bernstein and W. A. Seidler, Phys. Lett. 39B, 583 (1972); G. Alkhazov *et al.*, Phys. Lett. 57B, 47 (1975); G. Dugan, S. Childress, L. M. Lederman, L. E. Price, and T. Sanford, Phys. Rev. C 8, 909 (1973).

[4]B. W. Allardyce *et al.*, Nucl. Phys. A209, 1 (1973).

[5]W. M. Bugg, G. T. Condo, E. L. Hart, H. O. Cohn, and R. D. McCulloch, Phys. Rev. Lett. 31, 475 (1973); M. Leon and R. Seki, Nucl. Phys. B74, 68 (1974).

[6]L. O. Abramyan *et al.*, Yad. Fiz. 16, 739 (1973) [Sov. J. Nucl. Phys. 16, 412 (1973)]; M. Alvensleben *et al.*, Phys. Rev. Lett. 24, 792 (1970).

[7]J. W. Negele, in *Proceedings of the International Conference on Nuclear Structure and Spectroscopy, Amsterdam, The Netherlands, 1974*, edited by H. P. Blok and A. E. L. Dieperink (Scholar's Press, Amsterdam, 1974), p. 618.

[8]I. Sick, in *High Energy Physics and Nuclear Structure—1975*, AIP Conference Proceedings No. 26, edited by D. E. Nagle *et al.* (American Institute of Physics, New York, 1975), p. 388.

[9]G. C. Li, I. Sick, J. D. Walecka, and G. E. Walker, Phys. Lett. 32B, 317 (1970).

[10]T. W. Donnelly and J. D. Walecka, Nucl. Phys. A201, 81 (1973).

[11]G. H. Fuller and V. W. Cohen, Nucl. Data Tables 5, 457 (1971).

[12]P. Leconte, Ph.D. thesis, Saclay, 1976 (unpublished).

[13]I. Sick, J. B. Bellicard, M. Bernheim, B. Frois, M. Huet, P. Leconte, J. Mougey, Phan Xuan Hô, D. Royer, and S. Turck, Phys. Rev. Lett. 35, 910 (1975).

[14]I. Sick and J. S. McCarthy, Nucl. Phys. A150, 631 (1970).

[15]Code HEINEL of J. Heisenberg, modified for magnetic scattering.

[16]X. Campi, private communication.

[17]J. Negele, Phys. Rev. C 1, 1260 (1970).

[18]P. K. A. deWitt Huberts *et al.*, Phys. Lett. 60B, 157 (1976), and to be published.

[19]Meson-exchange corrections are expected to be unimportant near maxima of $F(q)$; we also note that because of the same magnitude and relative sign they should largely cancel in the Sr/Nb comparison. (T. W. Donnelly, private communication.)

[20]J. Decharge and D. Gogny, private communication.

Determination of Γ_n/Γ_f at 12 to 20 MeV Excitation from Evaporation-Residue Cross Sections*

P. D. Goldstone, H. C. Britt, R. Schoenmackers,† and J. B. Wilhelmy
Los Alamos Scientific Laboratory, University of California, Los Alamos, New Mexico 87545
(Received 15 April 1977)

Angular distributions of evaporation residues from the (^{7}Li,α) reaction on ^{197}Au, ^{232}Th, and ^{236}U have been measured as a function of excitation energy in the compound nuclei ^{200}Hg, ^{235}Pa, and ^{239}Np. Evaporation-residue probabilities $P_{ER} = \sigma(^7\text{Li},\alpha xn)/\sigma(^7\text{Li},\alpha)$ are obtained. These give the first microscopic information on Γ_n/Γ_f at 12 to 20 MeV excitation, which is independent of the compound-nucleus formation cross section. The results are compared with expectations based on previous systematic values of Γ_n/Γ_f.

The competition between fission and neutron emission in excited actinide nuclei has long been a subject of interest. Recently, reactions such as (^{3}He, *df*) have been used to provide measurements of the fission probability $P_f \equiv \langle \Gamma_f/(\Gamma_f + \Gamma_n + \Gamma_\gamma) \rangle$ in a variety of actinide nuclei for excitation energies from the barrier region up to ~12 MeV.[1,2] From these measurements Γ_n/Γ_f was determined as a function of excitation energy. Moreover, comparisons of P_f with the results of microscopic statistical model calculations have yielded information about fission barrier parameters[1,2] and the nuclear symmetries at the fission saddle points (e.g., evidence that the inner saddle point corresponds to axially deformed shapes).[1] It is desirable to extend measurements of Γ_n/Γ_f to ex-